



Contents lists available at ScienceDirect

Chinese Chemical Letters

journal homepage: www.elsevier.com/locate/ccl

Communication

Fluorescence enhancement and cytotoxicity reduction of bis-viologen biphenyl by complexation of cucurbit[7]uril



Jing Zhou^{a,b}, Shengzhen Hou^{a,b}, Jin Zhang^{a,b}, Yanru Chen^{a,b}, Hao Chen^{a,b,*},
Yebang Tan^{a,b,*}

^a School of Chemistry and Chemical Engineering, Shandong University, Ji'nan 250100, China

^b Key Laboratory of Special Functional Aggregated Materials, Ministry of Education, Shandong University, Ji'nan 250100, China

ARTICLE INFO

Article history:

Received 6 June 2020

Received in revised form 12 July 2020

Accepted 22 July 2020

Available online 25 July 2020

Keywords:

Cucurbit[7]uril

Host-guest complex

Fluorescence enhancement

Improvement of biocompatibility

ABSTRACT

The effect of cucurbit[7]uril (CB[7]) on fluorescence properties and biocompatibility of the bis-viologen biphenyl molecule (BPV2²⁺) was investigated by using ¹H NMR spectroscopy, fluorescence emission titration, and *in vitro* cytotoxicity experiments. CB[7] can be combined with BPV2²⁺ in a stoichiometric ratio of 1:1 and 2:1. After the formation of host-guest complex, the fluorescence emission intensity of BPV2²⁺ increased significantly, and the emission spectrum blue shifted. Meanwhile, the host-guest complexes showed better biocompatibility than BPV2²⁺ in cell cytotoxicity studies. Results of this paper lay a foundation for the development of host-guest type of fluorescent probes, biological imaging and so forth.

© 2020 Chinese Chemical Society and Institute of Materia Medica, Chinese Academy of Medical Sciences. Published by Elsevier B.V. All rights reserved.

Organic fluorescent materials have attracted much attention because of their potential applications in fluorescent sensors [1–3], light-emitting diodes [4–6], smart color-changing materials, fluorescent probes [7–9] and imaging agents in biological systems [10,11]. Organic fluorescent small molecules are an important way to obtain new luminescent materials. Due to the hydrophobic effect of organic chromophores in aqueous solution, most of the organic fluorescent small molecules are conjugated molecules with poor water solubility. However, the biological system is a relatively complex aqueous system. Therefore, it greatly hinders the application of organic fluorescent small molecules in fluorescence imaging [12]. Moreover, organic fluorescent molecules with aromatic rings have toxicity [13]. Therefore, it is a great challenge to obtain water-soluble organic fluorescent molecules with good biocompatibility and apply them in biomedical field.

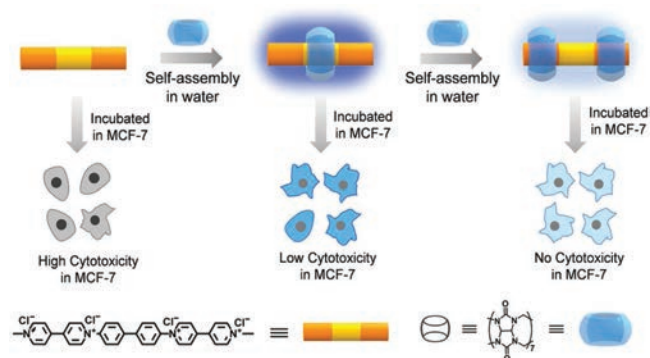
Supramolecular assembly can change the optical properties of fluorescent molecules in aqueous solution by simply changing the noncovalent interactions such as coordinative bonds [14–16], hydrogen bonding [17,18], electrostatic interactions [19–21], and host-guest interactions [22–24]. Cucurbit[7]uril (CB[7]) is a kind of macrocyclic host molecule containing seven glycoluril units bridged by methylene group, with a cavity diameter of 7.3 Å and

a portal diameter of 5.4 Å [25–29]. CB[7] can not only form inclusion complexes with some fluorescent molecules with high selectivity and high binding constant in aqueous solution, but also affect the optical properties of organic guest molecules through encapsulation [30–34]. Galoppini and coworkers investigated the effect of CB[7] encapsulation on the fluorescence and electrochemical properties of *p*-tolyl viologen, DTV²⁺ [32]. They found that the fluorescence emission intensity of the DTV²⁺@2CB[7] complexes was an order of magnitude higher than free DTV²⁺. Trabolsi and coworkers employed pseudorotaxanes that formed by CB[7] and a diamino-viologen linker condensed with an aromatic tri-aldehyde core to prepare polyrotaxanated covalent organic framework (COF) [35]. Under the excitation of 375 nm, the COF, TpVCB[7], showed bright blue luminescence with $\lambda_{\max} = 467$ nm, while the COF (TpV) without CB[7] showed very weak luminescence. With CB[7] encapsulation, the fluorescence emission intensity of TpVCB[7] is eight times higher than that of TpV. These enhancements are mainly due to the fact that CB[7] encapsulation limits the molecular torsion and increases the molecular rigidity.

Fluorescent molecules need good biocompatibility if they are to be used for biological applications requiring fluorescence, such as in fluorescent probes and sensors and in bio-imaging. However, there are few reports in the literature on the effect of host-guest interaction on the biocompatibility of fluorescent guest molecules. Scherman and coworkers reported the formation of the pyrene-viologen-CB[8] ternary complex. They controlled the release and

* Corresponding authors at: School of Chemistry and Chemical Engineering, Shandong University, Jinan 250100, China.

E-mail addresses: chenh@sdu.edu.cn (H. Chen), ybtan@sdu.edu.cn (Y. Tan).



Scheme 1. Schematic illustration of the assembly modes of BPV2²⁺ and CB[7].

encapsulation of viologen by controlling the association and dissociation of the supramolecular peptide amphiphile, to modulate the toxicity and non-toxicity of supramolecular system [36]. Zhang and his colleagues proposed a supramolecular chemotherapy. They employed dynamic CB[7]-mediated host-guest interaction to control the loading and releasing of antitumor drugs, so as to regulate the cytotoxicity of antitumor drugs and improve the efficiency of antitumor drugs [37,38]. Inspired by these work, we proposed that CB[7] can not only change the fluorescence performance of guest molecules, but also change the biocompatibility of fluorescent guest molecules, making it a wide application prospect in the field of biosensor.

In order to prove the above hypothesis, we synthesized the bis-viologen biphenyl molecule (BPV2²⁺) [39] and studied the effect of CB[7] on the fluorescence performance and biocompatibility of BPV2²⁺. Through CB[7] encapsulation, not only the fluorescence intensity of BPV2²⁺ increased significantly, but also the cytotoxicity of BPV2²⁺ decreased markedly (Scheme 1). After interaction with CB[7], BPV2²⁺ has no cytotoxicity at all. Our main objective is to reveal how host-guest interaction affects the fluorescent properties and the cytotoxicity of BPV2²⁺, expand the biological application value of fluorescent molecules, and make more molecules used for biological imaging and labeling. Our group has designed fluorescent molecular switch based on the host-guest interaction [40]. we can combine the above ideas to design an integrated component of diagnosis and treatment in the future.

The formation of the host-guest complexes was monitored by ¹H NMR titration in D₂O (Fig. 1 and Fig. S2 in Supporting information). The signals of protons sitting inside the CB[7] cavity undergo significant upfield shifts, and the signals of protons close

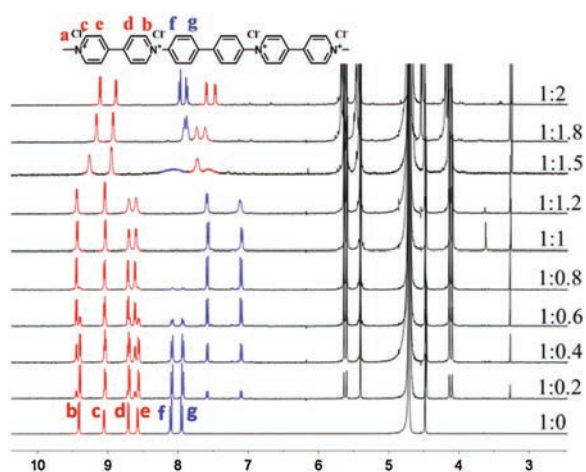


Fig. 1. ¹H NMR spectra of BPV2²⁺ with CB[7] in D₂O.

to the cavity portal, but not included, undergo a slight downfield shift. These characteristics provide important insight into the detection of the binding site of BPV2²⁺ with CB[7].

Upon addition of 1.0 equiv. of CB[7], the signals corresponded to the protons of the biphenyl moiety (H_f and H_g) shifted upfield by 0.52 and 0.86 ppm, whereas the signals of the viologen moiety protons (H_b, H_c, H_d and H_e) slightly shifted downfield by 0.02 ppm. The singlet associated with the methyl group (H_a) of BPV2²⁺ remained unchanged upon the addition of CB[7]. These results indicated that BPV2²⁺ could form a binary complex with CB[7], which resided on the biphenyl moiety. Upon addition of 2.0 equiv. of CB[7], the proton signals continued to change significantly except for the viologen moiety protons (H_a). The signals corresponded to the viologen moiety protons (H_d and H_e) shifted upfield by 1.10 ppm, whereas the signals of the viologen moiety protons (H_b and H_c) and biphenyl moiety (H_f and H_g) slightly shifted upfield by 0.31, 0.17, 0.12 and 0.08 ppm, respectively.

We can clearly see a remarkable broadening of the proton signals before the amount of CB[7] reached 2.0 equiv. (Fig. 1). A similar broadening of the ¹H NMR spectra for CB[7] complexes of viologens has been reported previously by Kaifer and coworkers [41,42]. A reasonable explanation for this phenomenon is that there is a dynamic change among species during the time scale of NMR observation [43]. This equilibria include shuttling the host between the viologen moiety and biphenyl moiety. The ¹H NMR peak of the BPV2²⁺@2CB[7] was sharper, and the extra amounts of CB[7] did not caused significant spectral changed, demonstrating the complexation was saturated with 2.0 equiv. of CB[7]. In summary, the ¹H NMR data indicated that different complexes formed when the ratio of BPV2²⁺ and CB[7] was different. The binary complex BPV2²⁺@CB[7] was formed upon addition of 1.0 equivalent of CB[7], however, a ternary complex BPV2²⁺@2CB[7] was formed upon addition of 2.0 equiv. of CB[7].

The binding properties of BPV2²⁺@CB[7] was studied using isothermal titration calorimetry (ITC). A titration curve was shown in Fig. 2a. The titration plot was fitted with two sets of sites model,

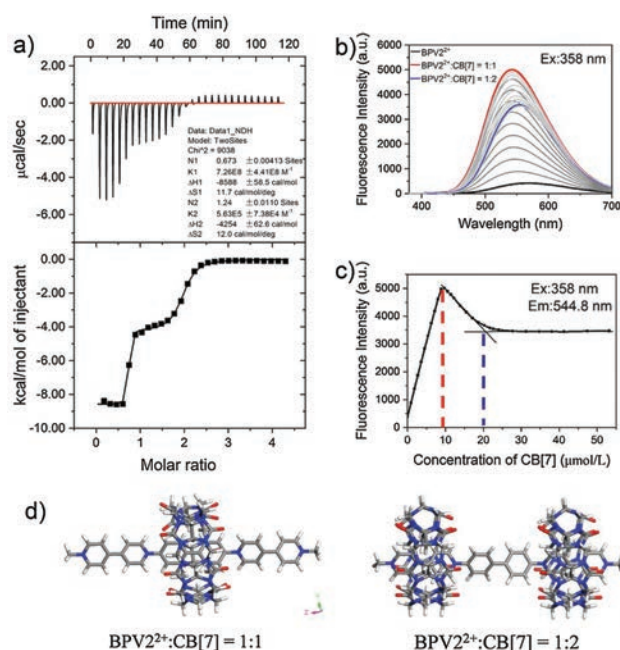


Fig. 2. (a) ITC titration plot of 2.0 mmol/L CB[7] with 0.1 mmol/L BPV2²⁺ at 298 K in H₂O. (b) Emission spectra of the titration of BPV2²⁺ (10 μmol/L) with CB[7] (0–200 μmol/L). (c) The fluorescence intensity at 544.8 nm with different amount of CB[7]. (d) Simulation model of the 1:1 and 2:1 complex of CB[7] and BPV2²⁺.

with first-step binding constant of $(7.26 \pm 4.41) \times 10^8$ L/mol and second-step binding constant of $(5.63 \pm 0.74) \times 10^5$ L/mol.

To further explore the interaction between BPV2²⁺ and CB[7], the fluorescence titration curves of BPV2²⁺ (10 μmol/L) with various CB[7] concentrations in aqueous solution were obtained. As shown in Fig. 2b, aqueous solution of BPV2²⁺ in the absence of CB[7] showed weak fluorescence. When an equivalent CB[7] was added, however, the emission spectra showed that the fluorescence emission intensity increased significantly, and the emission band blue shifted of 28 nm (λ_{em} from 571 nm to 543 nm). When two equivalent CB[7] were added, the fluorescence emission intensity decreased slightly, accompanied by the red shift of emission peak (λ_{em} from 542.8–553.8 nm). The titration curve of Fig. 2c showed that the fluorescence emission intensity reached maximum when the ratio of host to guest was 1:1, and the fluorescence emission intensity no longer changed when the ratio of host and guest reached 2:1. The results showed that the CB[7] encapsulation resulted in an order of magnitude enhancement of the fluorescence emission intensity.

This fluorescence intensity enhancement and blue shift of the emission induced by encapsulation of the guest molecule in a host has been reported in the literature [32]. This is mainly due to the following reasons. 1) The encapsulation of CB[7] increases the rigidity of the molecule and leads to a fluorescence enhancement. On the one hand, with the increase of rigidity, the intramolecular vibration is weakened, which makes the excitation energy of the molecule difficult to release in the form of thermal energy due to vibration. On the other hand, the increase of intramolecular vibration is weakened, which makes the excitation energy of the molecule difficult to release in the form of thermal energy due to vibration. On the other hand, the increase of rigidity is conducive to improving the coplanarity of molecules and fluidity of intramolecular π electrons. 2) The encapsulation of CB[7] can protect BPV2²⁺ from being quenched by solvent molecules. To better prove the above conclusion, the main dihedral distributions of BPV2²⁺ molecule were investigated in both free state and the complex state with CB[7]. The results of dihedral distributions were shown in Fig. 2d and Fig. S8 (Supporting information).

As shown in Table S1 (Supporting information), the fluorescence quantum yield of BPV2²⁺ was measured in water in the presence of different equivalents of CB[7]. The aqueous solution of BPV2²⁺ exhibited a low fluorescence quantum yield ($\Phi = 3.25\%$) in the absence of CB[7]. The fluorescence quantum yield and lifetime were significantly increased upon the addition of CB[7], depending on the ratio of BPV2²⁺ and CB[7]. When 1.0 equiv. of CB[7] was added, the maximum fluorescence quantum yield ($\Phi = 19.45\%$) was obtained, when 2.0 equiv. of CB[7] were added, the fluorescence quantum yield decreased slightly ($\Phi = 15.11\%$). The time-resolved experiments showed that the excited-state lifetime of BPV2²⁺ increased significantly from 0.05 ns to 1.04 ns upon encapsulation with 1.0 equiv. of CB[7] (Fig. S5 and Table S1). When CB[7] were added to 2.0 equiv., the excited-state decay kinetics of BPV2²⁺ displayed a long lifetime of 1.2 ns with a relatively short lifetime of 0.6 ns. The fluorescence decay profiles obey a biexponential function, proving the presence of two species in solution. For BPV2²⁺, the longer lifetime component of ~ 1.0 ns in aqueous solution was associated with the BPV2²⁺@CB[7], the shorter lifetime component of ~ 0.5 ns in aqueous solution was associated with the BPV2²⁺@2CB[7]. Due to the reversible assembly of BPV2²⁺@CB[7] and BPV2²⁺@2CB[7], there was a dynamic change among species. The contribution rate of BPV2²⁺@CB[7] was 45.7%, the contribution rate of BPV2²⁺@2CB[7] was 54.3%.

Upon addition of 1.0 equiv. of CB[7], the radiative decays rate had a mild change, from 19.95 s^{-1} to 0.18 s^{-1} , and the non-radiative decays rate was much slower, from 19.95 s^{-1} to 0.76 s^{-1} , calculated from the fluorescence quantum yield and lifetime. The latter were caused by a lack of fluorophore aggregation after encapsulation by

CB[7], and an inhibition of nonradiative relaxation by interaction with the solvent. Overall, the results indicated that the confinement in CB[7] primarily affects the rate of non-radiative energy dissipation processes of the singlet-excited BPV2²⁺.

To explore the effect of CB[7] encapsulation on the biocompatibility of BPV2²⁺, we used the MTT (3-(4,5-dimethylthiazol-2-yl)-2,5-diphenyltetrazolium bromide) assay to studied the *in vitro* toxicity of BPV2²⁺. MTT assays were performed after MCF-7 cells were incubated with different concentrations of BPV2²⁺ and BPV2²⁺@CB[7] and BPV2²⁺@2CB[7] for 48 h. Fig. 3 showed that when BPV2²⁺ was encapsulated in the CB[7] cavity, the cytotoxicity of BPV2²⁺ is low. After a 48 h incubation with 125 μmol/L BPV2²⁺, the viability of the cells was reduced to 28%, whereas for the BPV2²⁺@CB[7] and BPV2²⁺@2CB[7], the viability remained at 100%. At a 500 μmol/L loading concentration of BPV2²⁺, the cell viability reduced to 20%, the viability of BPV2²⁺@CB[7] was also reduced to 77%, and the activity of BPV2²⁺@2CB[7] was still maintained at 100%.

Some small molecules containing amines, amides, aromatic rings and pyridines tend to bind double-stranded DNA in different ways, including electrostatic adsorption and intercalation between base pairs. These interactions hinder the function of various enzymes and thereby induce toxicity to the living cells [44]. BPV2²⁺ is a toxic substance for humans and animals. We think that when BPV2²⁺ was encapsulated by 1.0 equiv. of CB[7], the host molecule prevented the insertion of BPV2²⁺ between the base pairs, but the viologen moiety still had electrostatic adsorption, so it still induced toxicity to living cells. When BPV2²⁺ was encapsulated by 2.0 equiv. of CB[7], its interaction with DNA was completely prevented, which had no effect on cell viability.

Based on the MTT results, 62.5 μmol/L BPV2²⁺ with various concentration of CB[7] were used for imaging experiments. To understand the ability of BPV2²⁺ to be internalized by cells, MCF-7 cells were incubated with BPV2²⁺, BPV2²⁺@CB[7] and BPV2²⁺@2CB[7] for 6 h, respectively, following by imaged with a confocal laser scanning microscopy (CLSM, Leica SP8). As Fig. 4 showed, there was a significant difference between BPV2²⁺ and BPV2²⁺@CB[7]. The image of BPV2²⁺ did not show obvious color, while the images of BPV2²⁺@CB[7] obtained show a bright blue emission in the cytoplasm of the cells without changing their morphologies. The image of BPV2²⁺@2CB[7] showed a relatively low-bright blue emission. The phenomenon was consistent with the change in the fluorescence emission intensity.

To further confirm the intracellular internalization and location of BPV2²⁺, cells incubated with BPV2²⁺ for 6 h were further treated by WGA, staining cell membrane. The CLSM image revealed that the BPV2²⁺ mainly located inside the cytoplasm other than the nuclei and membranes (Fig. 4), confirming the efficient internalization and release behavior of BPV2²⁺.

In summary, a bi-viologen rigid guest molecule BPV2²⁺ can form 1:1 or 1:2 inclusion compounds with CB[7] in aqueous solution.

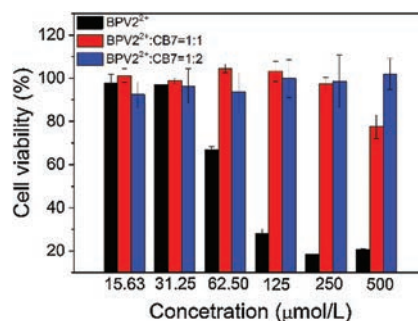


Fig. 3. Effect of different concentrations of BPV2²⁺, BPV2²⁺@CB[7], and BPV2²⁺@2CB[7] on MCF-7 cells viability after 48 h incubation. The cell viability was assessed using the MTT assay. The values presented are the mean \pm SD ($n = 3$).

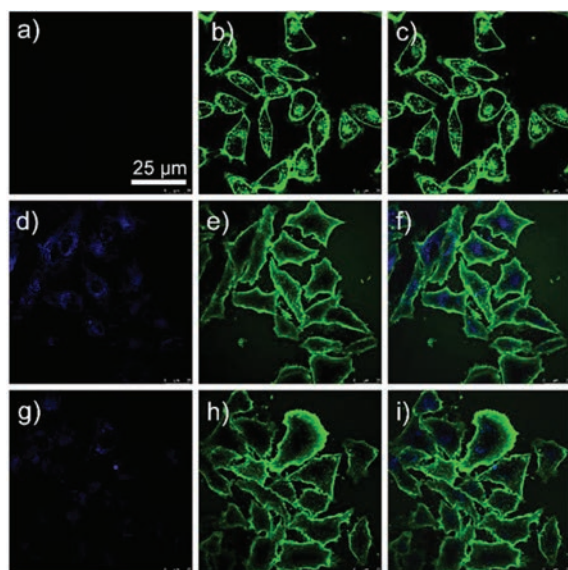


Fig. 4. Live-cell confocal microscopy images of MCF-7 cells. Cells were incubated with (a) BPV2²⁺, (d) BPV2²⁺@CB[7] and (g) BPV2²⁺@2CB[7] (62.5 μmol/L in PBS solution). (b, e, h) Cells were incubated with WGA. Cells were incubated with WGA and (c) BPV2²⁺ (f) BPV2²⁺@CB[7] and (i) BPV2²⁺@2CB[7]. Scale bars: 25 μm.

Upon encapsulated by 1.0 equiv. CB[7], the emission intensity of the BPV2²⁺@CB[7] complex was enhanced 1 order of magnitude ($\Phi = 19.45\%$, $\tau = 1.04$ ns) and blue-shifted by 28 nm. Upon encapsulated by 2.0 equivalent CB[7], the emission intensity of the BPV2²⁺@2CB[7] complex decreased ($\Phi = 15.11\%$, $\tau_1 = 1.2$ ns, $\tau_2 = 0.6$ ns). Meanwhile, the cytotoxicity of BPV2²⁺ was significantly reduced by the encapsulation of CB[7]. This remarkable enhancement of fluorescence intensity and biocompatibility makes BPV2²⁺ performed well in cell imaging, which holds promise for the application of fluorescent molecules in biological fields such as biological imaging and labeling.

Declaration of competing interest

The authors declare that they have no known competing financial interests or personal relationships that could have appeared to influence the work reported in this paper.

Acknowledgments

This work was supported by the National Natural Science Foundation of China (No. 21374055) and the Fundamental Research Funds of Shandong University (No. 11190078614092).

Appendix A. Supplementary data

Supplementary material related to this article can be found, in the online version, at doi:<https://doi.org/10.1016/j.cclet.2020.07.039>.

References

- [1] K.P. Carter, A.M. Young, A.E. Palmer, *Chem. Rev.* 114 (2014) 4564–4601.
- [2] D. Cao, H. Meier, *Chin. Chem. Lett.* 30 (2019) 1758–1766.
- [3] N. Yan, J. Song, F. Wang, *Chin. Chem. Lett.* 30 (2019) 1984–1988.
- [4] M.Y. Wong, E. Zysman-Colman, *Adv. Mater.* 29 (2017) 1605444.
- [5] M. Zhu, C. Yang, *Chem. Soc. Rev.* 42 (2013) 4963–4976.
- [6] J.H. Jou, S. Kumar, A. Agrawal, *J. Mater. Chem. C* 3 (2015) 2974–3002.
- [7] Y.L. Pak, K.M.K. Swamy, J. Yoon, *Sensors* 15 (2015) 24374–24396.
- [8] J.S. Kim, D.T. Quang, *Chem. Rev.* 107 (2007) 3780–3799.
- [9] Y. Luo, W. Zhang, M. Liu, et al., *Chin. Chem. Lett.* 32 (2021) 367–370.
- [10] S.K. Yang, X. Shi, S. Park, et al., *Nat. Chem.* 5 (2013) 692–697.
- [11] H. Lu, J. Mack, Y. Yang, et al., *Chem. Soc. Rev.* 43 (2014) 4563–4601.
- [12] M. De, P.S. Ghosh, V.M. Rotello, *Adv. Mater.* 20 (2008) 4225–4241.
- [13] X. Michalet, F.F. Pinaud, L.A. Bentolila, et al., *Science* 307 (2005) 538–544.
- [14] Q. Tang, S. Liu, Y. Liu, et al., *Inorg. Chem.* 53 (2013) 289–293.
- [15] M.S. Wang, G.C. Guo, *Chem. Commun.* 52 (2016) 13194–13204.
- [16] X. Yan, T.R. Cook, P. Wang, et al., *Nat. Chem.* 7 (2015) 342.
- [17] H. Wang, X. Ji, Z. Li, et al., *Mater. Chem. Frontiers* 1 (2017) 167–171.
- [18] D. Gonza'lez-Rodri'guez, A.P. Schenning, *Chem. Mater.* 23 (2010) 310–325.
- [19] K. Sakai, S. Tsuchiya, T. Kikuchi, et al., *J. Mater. Chem. C* 4 (2016) 2011–2016.
- [20] X.H. Jin, C. Chen, C.X. Ren, et al., *Chem. Commun.* 50 (2014) 15878–15881.
- [21] S. Bhattacharya, S.K. Samanta, *Chem. Eur. J.* 18 (2012) 16632–16641.
- [22] S.H. Li, X. Xu, Y. Zhou, et al., *Org. Lett.* 19 (2017) 6650–6653.
- [23] Y. Xia, S. Chen, X.L. Ni, *ACS Appl. Mater. Interfaces.* 10 (2018) 13048–13052.
- [24] E. Masson, M. Raiesi, K. Kotturi, *Isr. J. Chem.* 58 (2018) 413–434.
- [25] J. Kim, I.S. Jung, S.Y. Kim, et al., *J. Am. Chem. Soc.* 122 (2000) 540–541.
- [26] J.W. Lee, S. Samal, N. Selvapalam, et al., *Acc. Chem. Res.* 36 (2003) 621–630.
- [27] J. Lagona, P. Mukhopadhyay, S. Chakrabarti, L. Isaacs, *Angew. Chem. Int. Ed.* 44 (2005) 4844–4870.
- [28] A. Day, A.P. Arnold, R.J. Blanch, et al., *J. Org. Chem.* 66 (2001) 8094–8100.
- [29] D. Shetty, J.K. Khedkar, K.M. Park, et al., *Chem. Soc. Rev.* 44 (2015) 8747–8761.
- [30] H.J. Kim, W.S. Jeon, Y.H. Ko, K. Kim, *PNAS* 99 (2002) 5007–5011.
- [31] M. Freitag, E. Galoppini, *Langmuir* 26 (2010) 8262–8269.
- [32] M. Freitag, L. Gundlach, P. Piotrowiak, E. Galoppini, *J. Am. Chem. Soc.* 134 (2012) 3358–3366.
- [33] Z.L. Qian, X.H. Huang, Q.C. Wang, *Dye. Pigm.* 145 (2017) 365–370.
- [34] W. Wu, S. Song, X. Cui, et al., *Chin. Chem. Lett.* 29 (2018) 95–98.
- [35] G. Das, S.K. Sharma, T. Prakasam, et al., *Commun. Chem.* 2 (2019) 106.
- [36] D.Z. Jiao, J. Geng, X.J. Loh, et al., *Angew. Chem. Int. Ed.* 51 (2012) 9633–9637.
- [37] Y. Chen, Z. Huang, H. Zhao, et al., *ACS Appl. Mater. Interfaces.* 9 (2017) 8602–8608.
- [36] D.Z. Jiao, J. Geng, X.J. Loh, et al., *Angew. Chem. Int. Ed.* 51 (2012) 9633–9637.
- [37] Y. Chen, Z. Huang, H. Zhao, et al., *ACS Appl. Mater. Interfaces.* 9 (2017) 8602–8608.
- [38] Y. Chen, Z. Huang, J.F. Xu, et al., *ACS Appl. Mater. Interfaces.* 8 (2016) 22780–22784.
- [39] T.G. Zhan, T.Y. Zhou, F. Lin, et al., *Org. Chem. Front.* 3 (2016) 1635–1645.
- [40] H. Chen, H. Yang, W.C. Xu, et al., *Chin. Chem. Lett.* 24 (2013) 857–860.
- [41] K. Moon, A.E. Kaifer, et al., *Org. Lett.* 6 (2004) 185–188.
- [42] R. Wang, D. Bardelang, M. Waite, et al., *Org. Biomol. Chem.* 7 (2009) 2435–2439.
- [43] P. Montes-Navajas, A. Corma, H. Garcia, *J. Mol. Catalysis A: Chem.* 279 (2008) 165–169.
- [44] I. Roy, S. Bobbala, J. Zhou, et al., *J. Am. Chem. Soc.* 140 (2018) 7206–7212.